Structural Engineering and Mechanics, *Vol. 78, No. 3 (2021) 305-317*
DOI: https://doi.org/10.12989/sem.2021.78.3.305

Model reduction techniques for high-rise buildings and its reduced-order controller with an improved BT method

Chao-Jun Chen[1,2], Jun Teng[1], Zuo-Hua Li*[1], Qing-Gui Wu[1] and Bei-Chun Lin[1]

[1]School of Civil and Environmental Engineering, Harbin Institute of Technology, Shenzhen, Shenzhen, P.R. China
[2]Department of Civil and Environmental Engineering, The Hong Kong Polytechnic University, Hong Kong, P.R. China

(*Received February 14, 2020, Revised February 27, 2021, Accepted February 28, 2021*)

Abstract. An AMD control system is usually built based on the original model of a target building. As a result, the fact leads a large calculation workload exists. Therefore, the orders of a structural model should be reduced appropriately. Among various model-reduction methods, a suitable reduced-order model is important to high-rise buildings. Meanwhile, a partial structural information is discarded directly in the model-reduction process, which leads to the accuracy reduction of its controller design. In this paper, an optimal technique is selected through comparing several common model-reduction methods. Then, considering the dynamic characteristics of a high-rise building, an improved balanced truncation (BT) method is proposed for establishing its reduced-order model. The abandoned structural information, including natural frequencies, damping ratios and modal information of the original model, is reconsidered. Based on the improved reduced-order model, a new reduced-order controller is designed by a regional pole-placement method. A high-rise building with an AMD system is regarded as an example, in which the energy distribution, the control effects and the control parameters are used as the indexes to analyze the performance of the improved reduced-order controller. To verify its effectiveness, the proposed methodology is also applied to a four-storey experimental frame. The results demonstrate that the new controller has a stable control performance and a relatively short calculation time, which provides good potential for structural vibration control of high-rise buildings.

Keywords: flexible and high-rise buildings; active mass damper/driver; balanced truncation method; model reduction

1. Introduction

In order to suppress dynamic responses of civil engineering structures under external loads, an active mass damper/driver (AMD) (Bigdeli and Kim 2017, Xu *et al*. 2014, Zhang and Ou 2015, Zhu *et al*. 2012), an active tuned mass damper (ATMD) (Li *et al*. 2010, Li and Qu 2004, Li *et al*. 2009), a passive tuned mass damper (TMD) (Jiang *et al*. 2017, Mortezaie and Rezaie 2018, Li *et al*. 2019, Yang and Li 2017, Zhang *et al*. 2013), and other dampers (Qian *et al*. 2016, Zhang *et al*. 2014, Zhou and Huang 2018, Zhou *et al*. 2018) are commonly utilized. Indeed, the performance of an AMD system is better than other forms theoretically. However, several problems restrict the development of AMD systems. Specifically, high-rise buildings have an excessive number of degrees of freedom, and therefore the designed controller based on an original model has a long time-delay that is too difficult to fulfill the real-time control requirement (Pekar and Matusu 2018, Qu *et al*. 2014). Hence, it is important to build a reduced-order controller.

The primary problem of a reduced-order control system is summed up as the establishment of a reduced-order model. Model-reduction methods (Jin *et al*. 2014) are used to transform a relatively complex model into a simple reduced-order model. Model-reduction methods are usually used in engineering practice, such as balanced truncation method, dynamic condensation method, modal analysis reduction, etc. For instance, the elastic model-order reduction technique has been used to calculate contact forces due to impacts in hydraulic valves (Koreck and Von Estorff 2015). Based on a parametric model-order reduction, a coupled finite-element boundary-element method for solving parametric models of eddy-current problems has been proposed in reference (Klis *et al*. 2016). In reference (Azam and Mariani 2013), the performance of reduced order modeling of dynamic structural systems based on a proper orthogonal decomposition technique has been investigated, and then a reduced model through singular value decomposition and Galerkin projection has been built. In order to gain insight into the fluid flow physics, and potentially identify mechanisms for controlling these flows, reference (Rowley and Dawson 2017) has extracted simplified models based on balanced truncation and dynamic mode decomposition. According to eigenvalues' size of state vectors in a structure, balanced truncation method can reorder these state vectors to form the internal equilibrium model, while partial state vectors that correspond to the small eigenvalues will be omitted (Hartmann *et al*. 2010). A dynamic condensation method is an iterative method that uses an eigenvalue-shifting technique (Boo and Lee 2017). Compared with a static condensation method, the accuracy of the reduced-order model obtained from a dynamic condensation method is relatively higher, and it is easier to design a control system for a reduced-order system than for a full-order system

*Corresponding author, Associate Professor
E-mail: lizuohua@hit.edu.cn

http://www.techno-press.com/journals/sem&subpage=7
ISSN: 1225-4568 (Print), 1598-6217 (Online)

(Wang *et al*. 2015). In reference (Louca 2014), based on the modal analysis of multi-body systems, a new model-reduction method can be implemented to these systems with a non-proportional damping.

From the existing references, model-reduction methods are generally used in electronics, communications, aerospace and automation. Model-reduction technologies need to be further studied in civil engineering. Firstly, a suitable reduced-order model should be selected for high-rise buildings with a small first natural frequency, a large slenderness ratio and a high height (Shen *et al*. 2018). Then, a reduced-order controller is designed to reduce dynamic responses of high-rise buildings. Moreover, the calculation method of a control gain is particularly important. Conventional methods include a pole-assignment algorithm (Teng *et al*. 2016) and a linear quadratic regulator algorithm (Wang *et al*. 2009). However, they require an accurate mathematical model and cannot be used for uncertain systems. As a result, a suitable method called a regional pole-assignment algorithm is designed to consider the robustness in uncertain systems (Li *et al*. 2018).

In this paper, a suitable reduced-order model is selected for high-rise buildings after comparing the transfer functions of several reduced-order models corresponding to different methods, and then the influence of retained orders on the system performance is analyzed. Based on a suitable reduced-order model, a new reduced-order controller proposed for high-rise buildings is performed to reduce a long control-force calculation time. Finally, a real high-rise building and a four-storey experimental frame are presented to validate the effectiveness of the proposed method.

2. Establishment of several reduced-order models

2.1 Common reduced-order methods

The force equilibrium equation of a high rise building with an AMD system is

$$M_o\ddot{X}(t) + C_o\dot{X}(t) + K_oX(t) = B_w w(t) + B_s u(t) \tag{1}$$

where M_o, C_o and K_o are the mass, damping and stiffness matrices of the system, respectively. u and w are the control forces and the input excitations. B_s and B_w are the position matrices of the control forces and the input excitations. X is the displacements of the system, respectively.

Eq. (1) can be described as

$$\begin{cases} \dot{Z}(t) = AZ(t) + B_1 w(t) + B_2 u(t) \\ Y(t) = CZ(t) + D_1 w(t) + D_2 u(t) \end{cases} \tag{2}$$

where Z is the state vector that includes the displacements and the velocities. A, B_1 and B_2 are the state matrix, the excitation matrix and the control matrix, respectively. C, D_1 and D_2 are the state output matrix, the direct transmission matrices of the control forces and the external excitations, respectively. Y is the output vector.

The observation equation can output the displacements, the velocities, the accelerations and the control forces of the system. A, B_1, B_2, C, D_1 and D_2 can be expressed as

$$\begin{aligned} &A = \begin{bmatrix} 0 & I \\ -M_o^{-1}K_o & -M_o^{-1}C_o \end{bmatrix}, B_1 = \begin{bmatrix} 0 \\ -M_o^{-1}B_w \end{bmatrix}, B_2 = \begin{bmatrix} 0 \\ -M_o^{-1}B_s \end{bmatrix}, \\ &C = \begin{bmatrix} I & 0 \\ 0 & I \\ -M_o^{-1}K_o & -M_o^{-1}C_o \\ 0 & 0 \end{bmatrix}, D_1 = \begin{bmatrix} 0 \\ 0 \\ -M_o^{-1}B_w \\ 0 \end{bmatrix}, D_2 = \begin{bmatrix} 0 \\ 0 \\ -M_o^{-1}B_s \\ 1 \end{bmatrix}. \end{aligned} \tag{3}$$

2.1.1 An improved balanced truncation method

A balanced truncation (BT) method is a process that the original control system can be transformed into a balanced realization system by a non-singular transformation, and then truncates the balanced realization system according to the singular value of a Hankel matrix.

Defining

$$Z(t) = TZ_b(t) \tag{4}$$

where T is the transform matrix. Z_b is the state vector of the balanced realization system.

By substituting Eq. (4) into Eq. (2), the state-space equation of the balanced realization system is

$$\begin{cases} \dot{Z}_b(t) = A_b Z_b(t) + B_{b1} w(t) + B_{b2} u(t) \\ Y_b(t) = C_b Z_b(t) + D_{b1} w(t) + D_{b2} u(t) \end{cases} \tag{5}$$

where $A_b = T^{-1}AT$, $B_{b1} = T^{-1}B_1$, $B_{b2} = T^{-1}B_2$, $C_b = CT$, $D_{b1} = D_1$ and $D_{b2} = D_2$.

According to reference (Laub *et al*. 1987), the transform matrix T is calculated as

$$T = L_c V S^{-1/2} \tag{6}$$

where V and S are the orthogonal and the positive diagonal matrices that can be obtained by applying the singular value decomposition technique for the matrix $L_o^T L_c$. L_c and L_o are the lower triangular matrices of the controllability and observability matrices decomposed by Cholesky.

Then the matrix S can be described as

$$S = \mathrm{diag}(\sigma_1, \sigma_2, \cdots, \sigma_n) \tag{7}$$

where σ_i is the diagonal elements that reflect the controllability and the observability of the state vector.

The diagonal elements σ_i were rearranged in descending order. When $\sigma_{r+1} << \sigma_r$, r is the retained orders and is the twice number of the structure vibration modes, it means that the states Z_{r+1}~Z_n corresponding to the eigenvalues σ_{r+1}~σ_n have a low performance of the controllability and the observability. Only the states Z_1~Z_r is retained in the balanced realization system. The state-space equation of this system is

$$\begin{cases} \dot{Z}_{br}(t) = A_{br} Z_{br}(t) + B_{br1} w(t) + B_{br2} u(t) \\ Y_{br}(t) = C_{br} Z_{br}(t) + D_{br1} w(t) + D_{br2} u(t) \end{cases} \tag{8}$$

where $A_{br} = A_b(1{:}r, 1{:}r)$, $B_{br1} = E_{b1}(:,\ 1{:}r)$, $B_{br2} = B_{b2}(1{:}r, :)$, $C_{br} = C_b(:,\ 1{:}r)$, $D_{br1} = D_{b1}$, $D_{br2} = D_{b2}$.

The truncation error of the reduced-order model shown as Eq. (8) can be defined as

$$\|e\|_\infty \le 2(\sigma_{r+1} + \sigma_{r+2} + \cdots + \sigma_n) \tag{9}$$

Depending on inequality (9), the model-reduction accuracy of the reduced-order model is

$$\eta = 1 - \|e\|_\infty / \left(2\sum_{i=1}^{n} \sigma_i \right) \ge \eta_{\min} \tag{10}$$

where $\eta_{\min}$=90% is the minimum model-reduction accuracy.

The model-reduction process of the BT method is only carried out on a partial small number of modes, which cannot guarantee the modeling accuracy. Its omitted state vectors decrease the accuracy of the reduced-order model. Therefore, it is necessary to re-consider this omitted modal information in the design process of a reduced-order controller.

The balanced realization system (8) is described as a block matrix.

$$\begin{cases} \begin{Bmatrix} \dot{Z}_{br}(t) \\ \dot{Z}_{bl}(t) \end{Bmatrix} = \begin{bmatrix} A_{br} & A_{b12} \\ A_{b21} & A_{b22} \end{bmatrix} \begin{Bmatrix} Z_{br}(t) \\ Z_{bl}(t) \end{Bmatrix} + \begin{Bmatrix} B_{br1} \\ B_{bl1} \end{Bmatrix} w(t) + \begin{Bmatrix} B_{br2} \\ B_{bl2} \end{Bmatrix} u(t) \\ Y_b(t) = \begin{bmatrix} C_{br} & C_{bl} \end{bmatrix} \cdot \begin{Bmatrix} Z_{br}(t) \\ Z_{bl}(t) \end{Bmatrix} + D_{b1} w(t) + D_{b2} u(t) \end{cases} \tag{11}$$

where Z_{br} and Z_{bl} are the retained, abandoned state vectors respectively.

Because the abandoned state vector Z_{bl} corresponding to the relatively small eigenvalues contains some vibration information, the process reduces the accuracy of order reduction.

Let

$$\begin{aligned} \dot{Z}_{bl}(t) = A_{b21} \cdot Z_{br}(t) + A_{b22} \cdot Z_{bl}(t) + B_{bl1} \\ \cdot w(t) + B_{bl2} \cdot u(t) = 0 \end{aligned} \tag{12}$$

Under an input excitation, the low-order modal mass participation ratio of a high-rise building is close to 1, and the high-order modal mass participation ratio is relatively small. Therefore, the contribution of high-order modes to the structural response can be ignored, and the structural responses corresponding to the high-order modes are assumed as zero, in order to fulfill the engineering requirement.

$$Z_{bl}(t) = -A_{b22}^{-1} \left[A_{b21} \cdot Z_{br}(t) + B_{bl1} \cdot w(t) + B_{bl2} \cdot u(t) \right] \tag{13}$$

Substituting Eq. (13) into Eq. (11) leads to

$$\begin{cases} \dot{Z}_{br}(t) = (A_{br} - A_{b12}A_{b22}^{-1}A_{b21})Z_{br}(t) + \\ \qquad (B_{br1} - A_{b12}A_{b22}^{-1}B_{bl1})w(t) + \\ \qquad (B_{br2} - A_{b12}A_{b22}^{-1}B_{bl2})u(t) \\ Y_{br}(t) = (C_{br} - C_{bl}A_{b22}^{-1}A_{b21})Z_{br}(t) \\ \qquad +(D_{b1} - C_{bl}A_{b22}^{-1}B_{bl1})w(t) \\ \qquad +(D_{b2} - D_{bl}A_{b22}^{-1}B_{bl2})u(t) \end{cases} \tag{14}$$

From the above improvement process, a new reduced-order system retains more information of the original system and reflects its dynamic characteristics accurately.

2.1.2 A dynamic condensation method

A dynamic condensation (DC) Method is based on structural vibration characteristics. The reduced-order control system is

$$M_r \ddot{X}(t) + C_r \dot{X}(t) + K_r X(t) = F_r(t) \tag{15}$$

where

$$\begin{cases} M_r = T^T M T, C_r = T^T C T \\ K_r = T^T K T, F_r(t) = T^T F(t) \\ T = \begin{bmatrix} I & R \end{bmatrix}, F(t) = \begin{bmatrix} B_w & B_s \end{bmatrix} \begin{bmatrix} w(t) \\ u(t) \end{bmatrix} \\ R = D_{ss}^{-1} \left[(M_{sm} + M_{ss} R) M_r^{-1} D_r - D_{sm} \right] \\ D = K - qM, D_r = K_r - qM_r \\ s = n - m, q = (\omega_{\min}^2 + \omega_{\max}^2)/2 \end{cases} \tag{16}$$

where the subscripts m and s are the master and the slave degrees of freedom of the system, respectively. The subscript r refers to the reserved model having m degrees of freedom. $[\omega_{\min}, \omega_{\max}]$ is a given frequency range. D_{ss}, D_{sm}, M_{ss} and M_{sm} are the sub-matrices of D and M, respectively, i.e., from

$$D = \begin{bmatrix} D_{mm} & D_{ms} \\ D_{sm} & D_{ss} \end{bmatrix}, M = \begin{bmatrix} M_{mm} & M_{ms} \\ M_{sm} & M_{ss} \end{bmatrix} \tag{17}$$

2.1.3 A modal value method

The modal analysis of a control system is widely used to study its behavior and relative controller design. After that, a modal value (MV) method is proposed to reduce the orders of high-rise buildings by a transformation matrix composed of relatively high value corresponding to vibration modes. The force equilibrium equation of a high-rise building with n degrees of freedom is shown as Eq. (1), and the system output is

$$Y = aX + b\dot{X} \tag{18}$$

where a and b are the output matrices.

The modal vector is

$$\phi = \{ \phi_1 \quad \phi_2 \quad \cdots \quad \phi_n \} \tag{19}$$

The vector in generalized coordinates is

$$q = \{ q_1 \quad q_2 \quad \cdots \quad q_n \}^T \tag{20}$$

Supposing

$$X = \phi q \tag{21}$$

Eqs. (1) and (18) are decoupled and transformed as

$$\begin{cases} \ddot{q} + (M^*)^{-1} C^* \dot{q} + (M^*)^{-1} K^* q = (M^*)^{-1} B^* U \\ Y = a^* q + b^* \dot{q} \end{cases} \tag{22}$$

where $M^* = \phi^T M_o \phi$, $C^* = \phi^T C_o \phi$, $K^* = \phi^T K_o \phi$, $B^* = \phi^T B$, $a^* = a\phi$ and $b^* = b\phi$.

As

$$(M^*)^{-1} C^* = \left[2\xi^* \omega^* \right], (M^*)^{-1} K^* = \left[(\omega^*)^2 \right] \tag{23}$$

Hence,

$$\begin{cases} \ddot{q}_i + 2\xi_i \omega_i \dot{q}_i + \omega_i^2 q_i = \phi_i^T B^* U / m_i \\ y_i = (a\phi_i) q_i + (b\phi_i) \dot{q}_i \end{cases} \tag{24}$$

The i^{th} modal value is

$$V_{jk}^{i}=\sqrt{\int_{0}^{\infty}y_{i}^{2}\left(t\right)dt}=\frac{\left|\phi_{i}^{T}B_{j}^{*}\right|\left[\left(a_{k}\phi_{i}\right)^{2}+\omega_{i}^{2}\left(b_{k}\phi_{i}\right)^{2}\right]^{\frac{1}{2}}}{m_{i}\omega_{i}\sqrt{\xi_{i}\omega_{i}}} \tag{25}$$

where B_j is the j^{th} column of B. a_k and c_k are the k^{th} row of a and c.

If the input and output dimensions of the system are n_1 and n_2, the number of the i^{th} modal value is $n_1 \times n_2$, and its sum is the i^{th} modal value. The transformation matrix T is composed of the modal vectors corresponding to the relatively high values.

$$T=\left[\phi_1 \quad \cdots \quad \phi_m\right] \tag{26}$$

Then the model-reduction process is the same as the BT method.

2.1.4 A revised minimum information loss method

Based on the observable and controllable information, a revised minimum information loss (RML) method, which is applicable to a linear time-invariant system, is proposed for the conventional minimum information loss method. In system (2), the transformation matrix is taken as $T=L_o^{-1}$. Singular value decomposition is used to decompose the controllable matrix of the output model.

$$P_b=\left[U_1 \quad U_2\right]\begin{bmatrix}S_1 & 0\\ 0 & S_2\end{bmatrix}\begin{bmatrix}U_1^T\\ U_2^T\end{bmatrix} \tag{27}$$

where

$$\begin{cases}U_1U_1^T+U_2U_2^T=I, U_2\in R^{n\times r},\\ S_1=diag\left(\sigma_1^2, \quad \sigma_2^2, \quad \cdots \quad \sigma_r^2\right)>0\\ S_2=diag\left(\sigma_{r+1}^2, \quad \sigma_{r+2}^2, \quad \cdots \quad \sigma_n^2\right)>0\\ \sigma_1^2\geq\sigma_2^2\geq\cdots\geq\sigma_r^2\geq\cdots\geq\sigma_n^2>0\end{cases} \tag{28}$$

Let

$$\begin{cases}L_r=U_1^TL_o\\ T_r=L_o^{-1}U_1\left(U_1^TU_1\right)^{-1}\end{cases} \tag{29}$$

The reduced-order model is

$$\begin{cases}\dot{Z}_r=A_rZ_r+B_ru\\ Y=C_rZ_r+D_ru\end{cases} \tag{30}$$

where Z_r is the state vector of a reduced- order model. A_r, B_r, C_r and D_r are the coefficient matrices with appropriate dimensions in a reduced-order model, respectively, which can be expressed as

$$A_r=L_rAT_r, B_r=L_rB, C_r=CT_r, D_r=D \tag{31}$$

From the model-reduction process of a high-rise building, the dimensionality of the matrices U_1 and U_2 determines the dimensionality of its reduced-order model and the state of its original model, while the dimensionalities of the matrices U_1 and U_2 have no quantitative constraint.

Table 1 The modal frequencies and the modal mass participation ratios of the ten-storey frame

Mode number	Modal frequencies (Hz)					Modal mass participation ratio
	Original model	BT	DC	MV	RML	
1	0.4140	0.4140	—	0.4140	0.1019	0.7829
2	1.2468	1.2468	—	1.2468	—	0.1124
3	2.2771	2.2771	1.8885	2.2771	—	0.0423
4	3.5032	3.5032	—	3.5032	—	0.0245
5	5.0239	5.0303	4.6242	5.0223	—	0.0144
6	6.8838	—	—	—	6.3710	0.0095
7	8.9331	—	8.4793	—	9.6513	0.0062
8	11.1545	—	—	—	—	0.0023
9	13.8599	—	13.5510	—	13.1736	0.0042
10	19.1768	—	19.1624	—	18.9920	0.0014

2.2 Comparative analysis and comparison of reduced-order methods

In this paper, the mathematical model of a ten-storey frame along its minor-axis is used as an example to compare and analyze these above methods. The frame includes a two-span beam along the minor-axis and a four-span beam along the major-axis. The height of each floor is 3.6 m, and the length, the height and the width of the beams along the minor-axis and the major-axis are 6000 mm×500 mm×300 mm. The dimensions of the columns from the 1^{st} to 5^{th} floors are 500 mm×500 mm, and the dimensions of the columns from the 6^{th} to 10^{th} floors are 400 mm×400 mm. The thickness of the slabs is 80 mm. The above frame is built by reinforced concrete, and its damping ratio is set as 0.02.

Through the BT, DC, MV and RML methods, the key parameter of the reduced-order model which includes the structural frequencies and the modal mass participation ratios of different vibration modes are shown in Table 1. Different reduced-order models are designed by a simulink toolbox in Matlab. Regarding the above ten-storey frame, the displacement and acceleration transfer functions of the 10^{th} floor under different methods are shown in Fig. 1. In these figures, ORM means the structure retains an original model (20 retained orders), while others are the reduced-order model (10 retained orders) through different methods. Considering its structural frequency range, the part between 0.1Hz and 100Hz is shown in the figures.

From Fig. 1 and Table 1, the displacement transfer functions of the above reduced-order models are basically consistent with the original model at low frequency, which means that the model-reduction process can retain the low-order dynamic characteristics of the original model. It is noteworthy that when the frequency of control voltage is consistent with the natural frequency of the frame, a sudden change of the magnitude transfer function is generated, and a resonance phenomenon between the structure and its controller occurs.

The reduced-order model obtained by the BT method or the MV method retains the first five modes of the original structure, which is continuous and has a relatively large modal mass participating ratio. Based on its structural

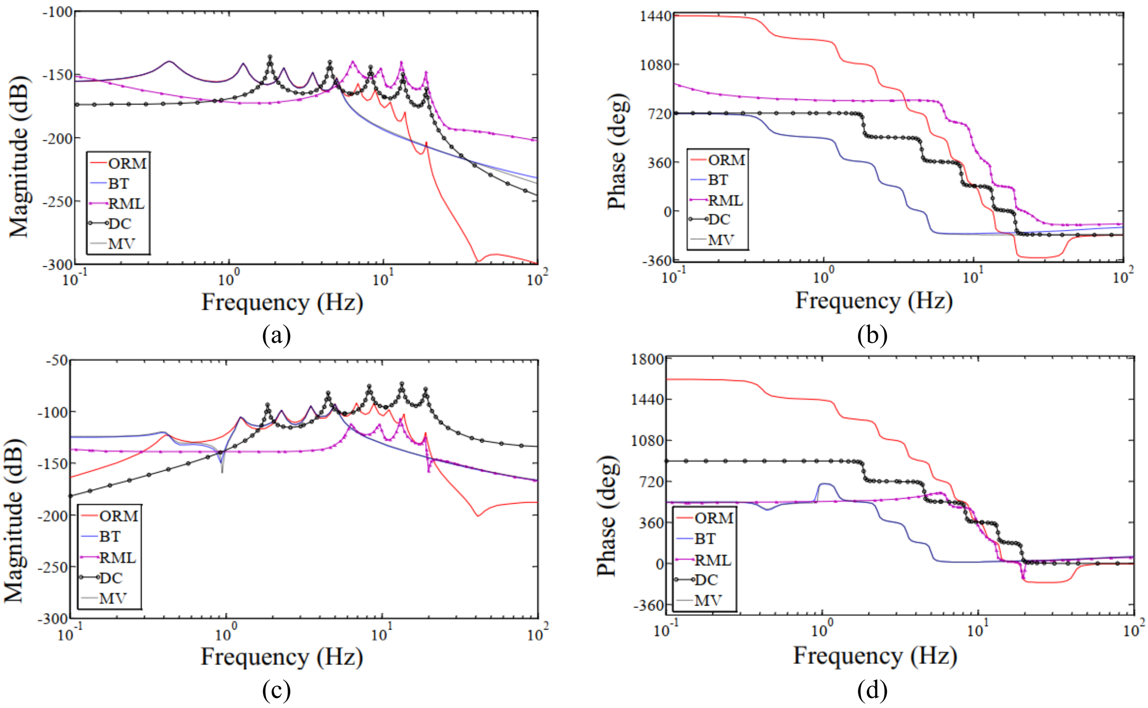

Fig. 1 The transfer functions of the 10th floor of different reduced-order models, (a) the magnitude and (b) the phase of the displacement transfer functions, (c) the magnitude and (d) the phase of the acceleration transfer functions

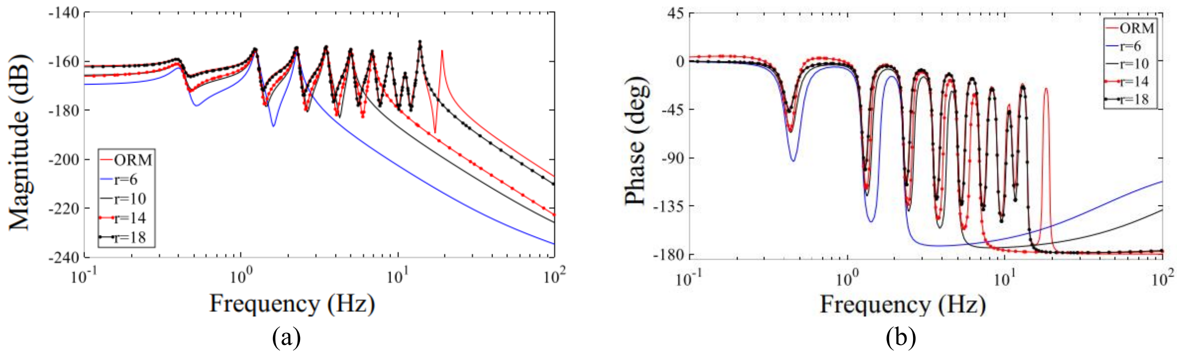

Fig. 2 The displacement transfer functions of the bottom floor under the BT method, (a) the magnitude and (b) the phase

vibration modes, the BT method that reduces the orders of a control system has a similar principle with the MV method. Through the MV method, several structural vibration modes with a high modal value are selected to obtain a reduced-order model. On the other hand, the difference between the original model and the model obtained by the BT method or the MV method is relatively smaller than that by the DC method or the RML method. The reduced-order model obtained by the DC method or the RML method retains the high-order modes of the original model which has a relatively small modal mass participating ratio, and the result causes the loss of its low-order characteristics. Generally, the dynamic characteristics of civil engineering structures are controlled by their low-order vibration modes. Therefore, the DC method or the RML method is unsuitable for civil engineering structures. The paper focuses on the BT method and combines it with the dynamic characteristics of high-rise buildings.

Based on the BT method, the above ten-storey frame structure is regarded as an example to analyze the influence of the number of the retained orders. The magnitudes of the displacement transfer functions of the bottom floor of its reduced-order models are shown in Fig. 2. In this figure, ORM means the structure retains the original model (20 orders), while r is the retained orders of 6, 10, 14 and 18. Considering the structural frequency range, the part between 0.1 Hz and 100 Hz is shown in the Fig. 2.

From Fig. 2, with the increase of the retained orders, the difference between the original model and the reduced-order model becomes smaller. The dynamic characteristics of the building are mainly determined by the first few modes of the original model that is continuous and with a large modal mass participating ratio. For the above frame, it is suggested to take 10 retained orders which mean the first five modes of the frame are retained (the modal mass participation ratio is 0.9765). The displacement transfer functions of the reduced-order model are basically consistent with the original model at low frequency which indicates that the dynamic characteristics of the original model are retained completely.

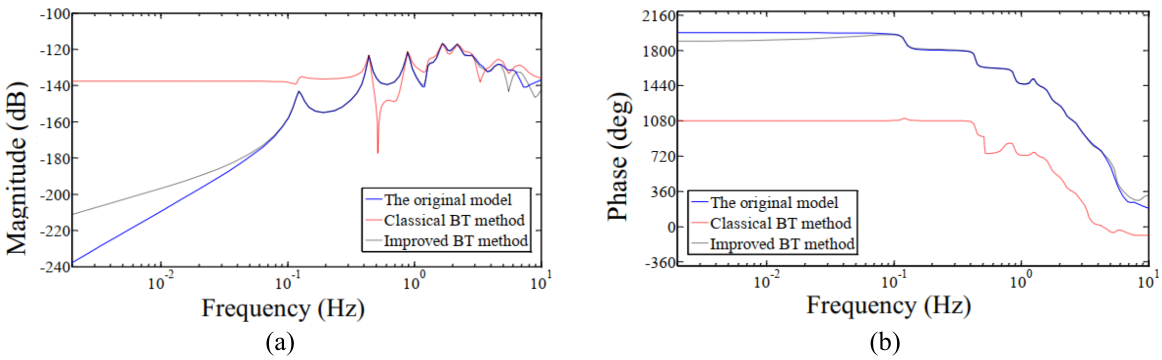

Fig. 3 The acceleration transfer functions of the 91st floor of the original model and the reduced-order models, (a) the magnitude and (b) the phase

Table 2 The natural periods of the original model and the reduced-order models

Mode number	The original model	The classical BT method		The improved BT method	
	Period (s)	Period (s)	Error (%)	Period (s)	Error (%)
1	7.1522	7.1522	0	7.1522	0
2	1.9435	1.9436	-0.2779	1.9435	0
3	0.9635	0.9455	1.8682	0.9543	0.9548
4	0.6467	0.6568	-1.5618	0.6512	-0.6958

3. Numerical verification

3.1 Influence analysis of the reduced-order model with an improved BT method

In this paper, a high-rise building called the KingKey Financial Center (KK100) (Chen *et al*. 2017) along its minor-axis is used as an example to compare and analyze these above methods which include the classical BT method and the improved BT method (in section 2.1.1). The orders of the original model and the reduced-order model are 202 and 50 respectively. The first twenty-five vibration modes of the building are retained, and the modal mass participation ratio is 0.9929, while the minimum model-reduction accuracy is 90%. Through the reduced-order process, the first four natural periods of different systems are compared in Table 2. Compared with the reduced-order model obtained by the classical BT method, the fundamental period or the second-order period of the reduced-order model obtained by the improved BT method is closer to that of the original model. With the increase of the orders, the difference between the natural periods of the reduced-order model and those of the original model become larger, indicating that the model-reduction process preserves the low-frequency natural vibration characteristics of the original model.

Regarding the above building, its acceleration transfer functions of the 91st floor are shown in Fig. 3. Considering the structural frequency range, the part between 0.01 Hz and 10 Hz is shown in the figures. From Fig. 3, the transfer functions of the two reduced-order models are basically consistent with the original model at high frequency, while the acceleration transfer function of the reduced-order model obtained by the classical BT method is not consistent well with the original model at low frequency. The reason is that the acceleration response is mainly affected by the higher modes and the reduced-order model obtained by the classical BT method discards the structural information of its high-order modes. Nevertheless, since the improved BT method presented in this paper retains the discarded information, its acceleration transfer function is basically consistent with the original model at low frequency, meaning the reduced-order model obtained by the improved BT method reflects the dynamic characteristics of the original model.

According to reference (Chen *et al*. 2017), a ten-year return period fluctuating wind load is generated for KK100. The speed is based on a Davenport spectrum, and a mixed autoregressive-moving average (MARMA) model is used to simulate the stochastic process of the wind load. Under the fluctuating wind load, the dynamic responses of the 87th floor between the original model and the reduced-order models of KK100 are shown in Fig. 4, respectively. **Error** is defined as the difference between the structural responses from the original model and the reduced-order model. From Fig. 4, the maximum variations of the displacement and acceleration responses between the original model and the reduced-order model obtained by the classical BT method is 0.7285×10^{-4} m, 0.0153 m/s^2, respectively. And the maximum variations of the displacement and acceleration responses between the original model and the reduced-order model obtained by the improved BT method is only 0.4460×10^{-7} m, 0.0354×10^{-2} m/s^2 which are all less than the former. Therefore, the precision of the reduced-order model obtained by the improved BT method is higher than that obtained by the classical BT method. Moreover, as the model-reduction process retains the low-order dynamic characteristics of the original model, while the acceleration responses are greatly affected by high-order dynamic characteristics, the maximum variations of the acceleration responses are more obvious than that of the displacement responses.

The displacement and acceleration responses along height between the original model and the reduced-order models are shown in Fig. 5. From Fig. 5, the dynamic responses of the reduced-order models are basically close to that of the original model. The error of the displacement responses of two reduced-order models is smaller than that of the acceleration responses. Obviously, the errors of the

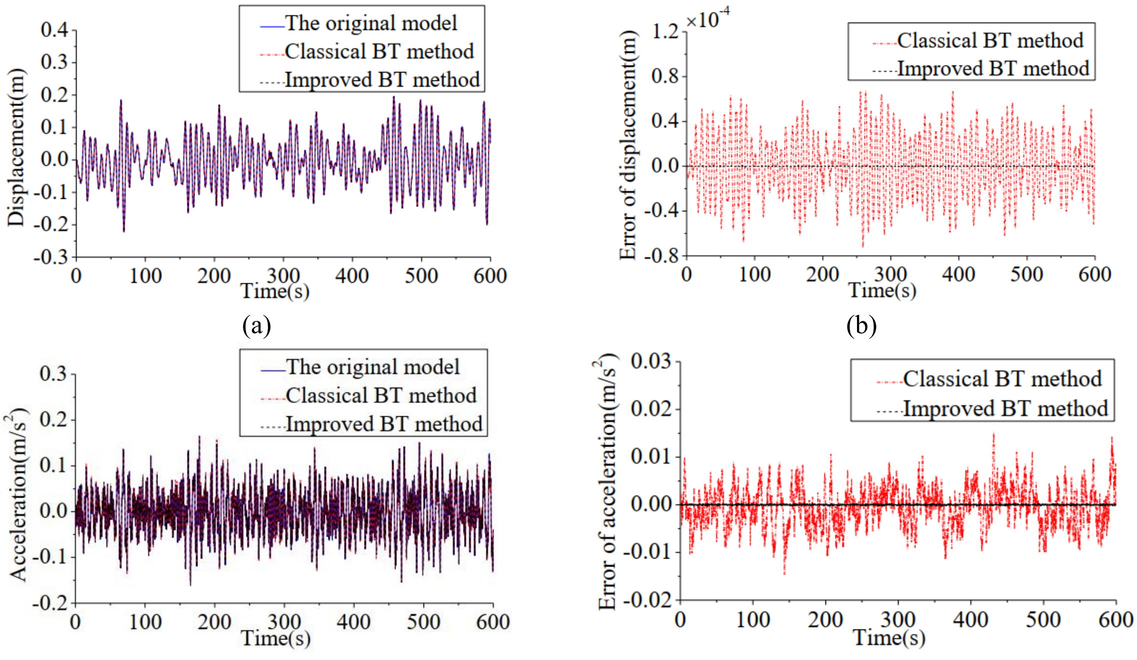

Fig. 4 The comparison of the structural responses of the 87th floor of KK100, (a) the displacement, (b) the errors of displacement, (c) the acceleration, (d) the errors of acceleration

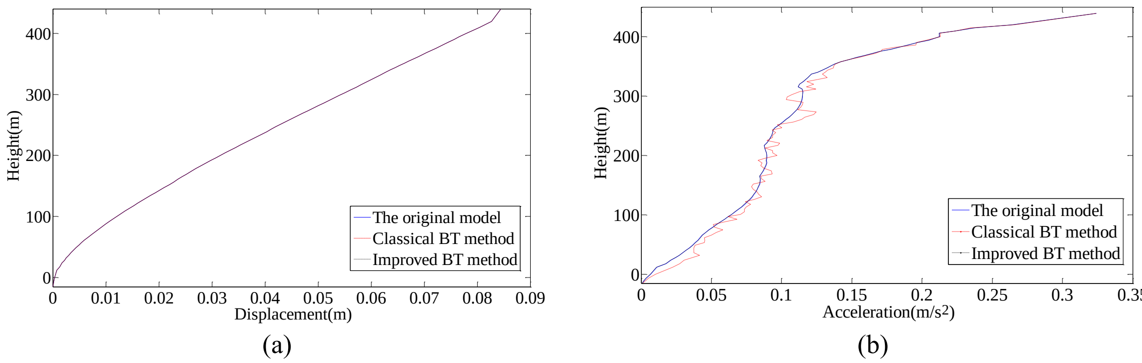

Fig. 5 The comparison of the structural responses along height, (a) the displacement, (b) the acceleration

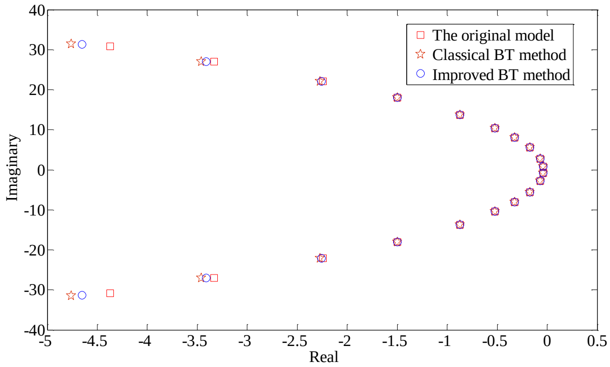

Fig. 6 The poles of the original model and the reduced-order models

reduced-order model obtained by the improved BT method are smaller than that of the classical BT method. The results reflect the superiority of the improved BT method. The improved BT method is more suitable to be used in reducing the orders of high-rise buildings.

The poles of different systems after using the original model and the reduced-order model obtained by the improved BT method are shown in Fig. 6. From Fig. 6, the pole positions of the balanced realization system are similar to those of the original system, indicating that the non-singular transformation does not change the system dynamic characteristics. The corresponding poles of the first eight modes before and after model-reduction generally coincide, indicating that the reduced-order system retains the information of the first eight modes of the original system. In addition, the first eight modal mass participation ratio of KK100 is 89.39% which is close to 90%, indicating that the controller design based on a reduced-order model meets the engineering requirement.

3.2 A reduced-order controller design

In the paper, a new controller is designed based on a reduced-order model obtained by the improved BT method. The control force of the reduced-order control system is

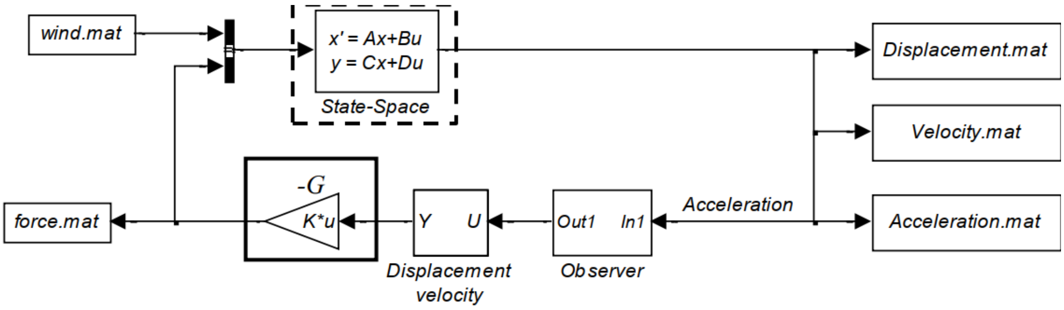

Fig. 7 The simulink block diagram of the reduced-order controller

$$u_{br}(t) = -G_{br} Z_{br}(t) \tag{32}$$

where G_{br} is a closed-loop feedback gain matrix.

Since the state vector Z_{br} cannot be observed directly, Eq. (4) is described as

$$Z_b(t) = T^{-1} Z(t) \tag{33}$$

Eq. (33) can be written as a block matrix.

$$\begin{Bmatrix} Z_{br}(t) \\ Z_{bl}(t) \end{Bmatrix} = \begin{bmatrix} (T^{-1})_{11} & (T^{-1})_{12} \\ (T^{-1})_{21} & (T^{-1})_{22} \end{bmatrix} \begin{Bmatrix} Z_1(t) \\ Z_2(t) \end{Bmatrix} \tag{34}$$

where Z_1 and Z_2 are the retained, abandoned state vectors corresponding to the original system.

Then

$$\begin{cases} Z_{br}(t) = (T^{-1})_{11} \cdot Z_1(t) + (T^{-1})_{12} \cdot Z_2(t) \\ Z_{bl}(t) = (T^{-1})_{21} \cdot Z_1(t) + (T^{-1})_{22} \cdot Z_2(t) \end{cases} \tag{35}$$

According to Eq. (35), Z_{bl} is

$$Z_{bl}(t) = (T^{-1})_{21} \cdot Z_1(t) + (T^{-1})_{22} \cdot Z_2(t) = 0 \tag{36}$$

From Eq. (36), Z_1 is

$$Z_2(t) = -\left[(T^{-1})_{22}\right]^{-1} \cdot (T^{-1})_{21} \cdot Z_1(t) \tag{37}$$

Substituting Eq. (37) into Eq. (34) leads to

$$Z_{br}(t) = \left\{(T^{-1})_{11} - (T^{-1})_{12} \cdot \left[(T^{-1})_{22}\right]^{-1} \cdot (T^{-1})_{21}\right\} \cdot Z_1(t) \tag{38}$$

Therefore, control force of the reduced-order control system shown in Eq. (32) is

$$\begin{aligned} u_{br}(t) = -G_{br} &\left\{(T^{-1})_{11} - (T^{-1})_{12}\right. \\ &\left.\cdot \left[(T^{-1})_{22}\right]^{-1} \cdot (T^{-1})_{21}\right\} \cdot Z_1(t) \end{aligned} \tag{39}$$

Let

$$G = G_{br} \left\{(T^{-1})_{11} - (T^{-1})_{12} \cdot \left[(T^{-1})_{22}\right]^{-1} \cdot (T^{-1})_{21}\right\} \tag{40}$$

Then the state feedback control law is

$$u_{br}(t) = -G \cdot Z_1(t) \tag{41}$$

Since the state vectors Z of a control system is estimated by the state observer in reference (Chen *et al*. 2017), the negative influence of observation errors is reduced by intercepting the first few state vectors. A regional pole-assignment method (Li *et al*. 2018) is applied in the AMD system. The simulink block diagram of the reduced-order controller is shown in Fig. 7. Its state-space equation is depicted by the dashed box, and the symbol inside the solid box in the figure represents the control gain obtained by the regional pole-assignment method.

Table 3 The control-force calculation time under different systems

Controller	The calculation time (s)	The accelerated ratio
The original controller	0.1847	--
The reduced-order controller	0.1356	26.58%

3.3 Numerical verification

Under a fluctuating wind load, the structural responses of the 87th floor and the AMD parameters of different control systems are shown in Fig. 8. The statement whether the reduced-order system can effectively reduce the time delays for calculating control forces is given in the part, and the control-force calculation time under different systems is shown in Table 3. The corresponding control effects and the AMD parameters are listed in Table 4. The **reduction** is defined as the ratio between structural response reduction and the responses without control, and the **AMD parameters** include control forces and strokes. The duration of each scenario is 600s, and Table 4 presents the root mean square values of the data.

From Fig. 8, Tables 3-4, the original controller and the reduced-order controller reduces wind vibration responses obviously, and the control effects and the AMD parameters of the reduced-order control system are close to the original control system. Specifically, the variations of the acceleration control effects of the 87th and 91st floors are only 0.0994% and 0.0899%. The AMD parameters of the reduced-order controller only increase by 0.0557 kN and 0.0001 m. In addition, the reduced-order controller can be used to instead of the original controller. The control-force calculation time of the original controller is 0.1847s. Nevertheless, the control-force calculation time of the reduced-order system with 50 retained orders is only 0.1356s. The accelerated ratio between the two systems is 26.58% which proved that the reduced-order controller not only guarantees the performance of the control system, but

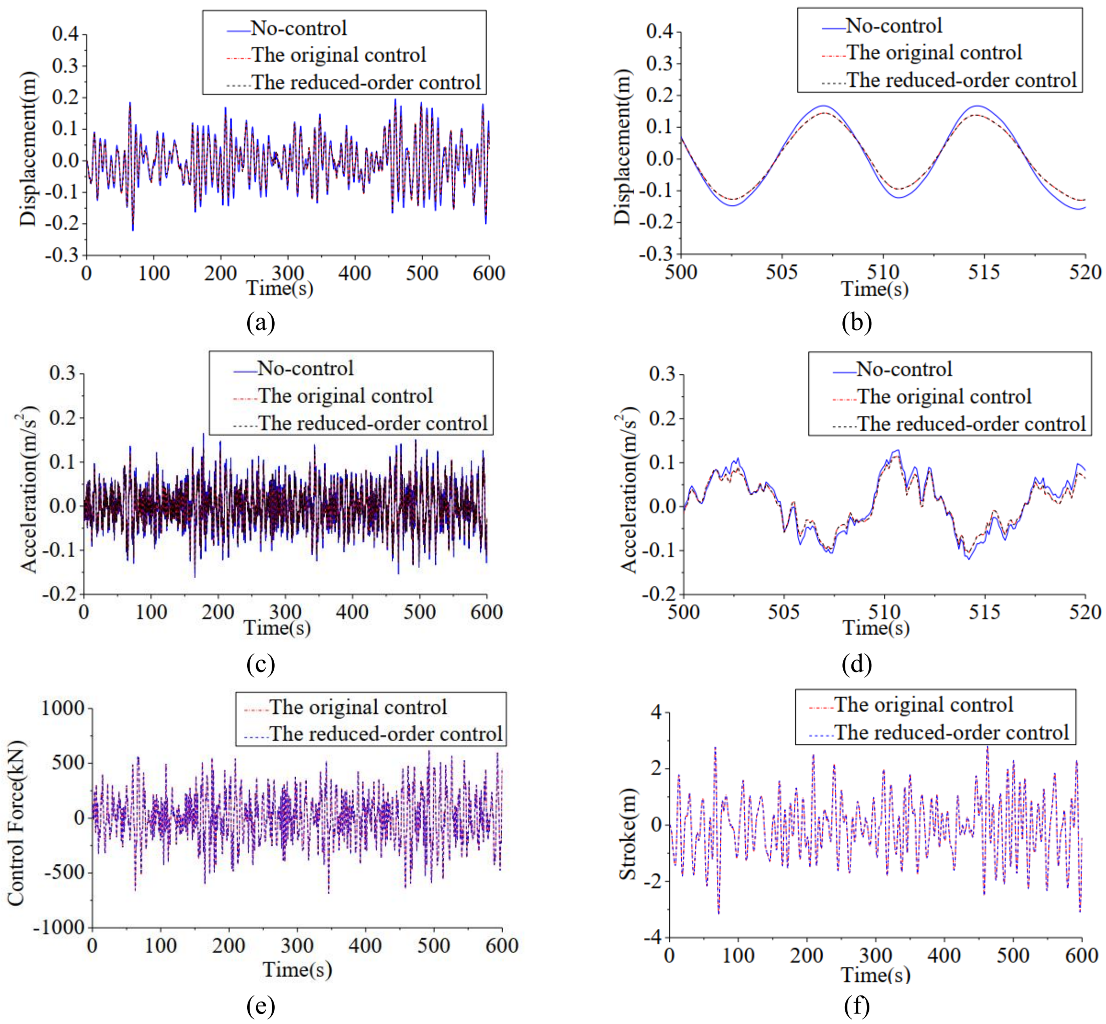

Fig. 8 The comparison of the structural responses of the 87th floor and the AMD parameters of KK100, the displacement (a) 0-600s and (b) 500-520s, the acceleration (c) 0-600s and (d) 500-520s, (e) the control force, (f) the stroke

Table 4 The responses of different control systems

Floor	Index	No-control	The original control		The reduced-order control	
			Response	Reduction (%)	Response	Reduction (%)
87th	Maximum displacement (m)	0.2594	0.2249	13.2999	0.2249	13.2999
	Maximum acceleration (m/s^2)	0.2011	0.1718	14.5699	0.1716	14.6693
91st	Maximum displacement (m)	0.2711	0.2351	13.2792	0.2351	13.2792
	Maximum acceleration (m/s^2)	0.2226	0.1891	15.0494	0.1893	14.9595
Maximum control force (kN)		—	620.0941	—	620.0384	—
Maximum stroke (m)		—	3.1625	—	3.1624	—

also reduces its control-force calculation time effectively.

Based on an energy conservation law, the energy equilibrium of a control system is

$$E_k + E_d + E_p = E_w + E_{AMD} \tag{42}$$

where E_k, E_d and E_p are the kinetic energy, the damping dissipation energy and the elastic potential energy of a high-rise building, respectively. E_w and E_{AMD} are the energy input from a wind load excitation and an auxiliary mass.

Based on Eq. (42), the kinetic energy, the damping dissipation energy and the elastic potential energy of the reduced-order model and the original model are shown in Figs. 9-11. The energy distribution of the reduced-order control system is shown in Fig. 12.

From these figures, the energy distribution of the reduced-order system is basically close to those of the original system. From the perspective of the energy distribution, a similar trend exists between the reduced-order system and the original system. Since a control system exerts energy on a controlled building, the damping dissipation energy of the system is greater than the external energy input. The damping dissipation energy is obviously greater than the kinetic energy and the elastic potential energy in a whole system which indicates that an AMD

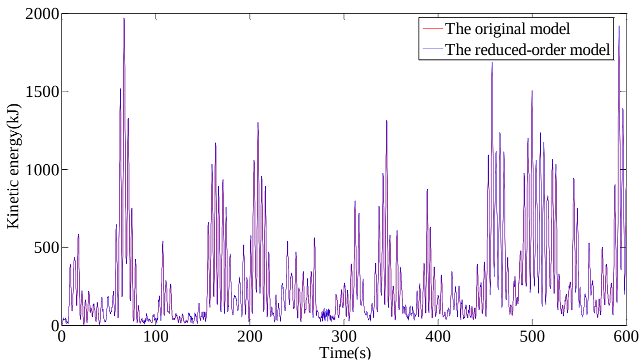

Fig. 9 The total kinetic energy of KK100

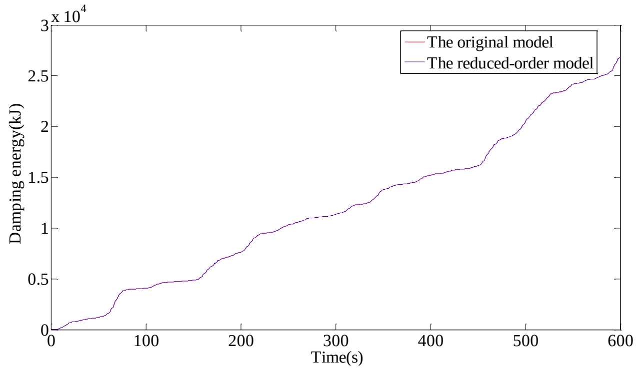

Fig. 10 The total damping dissipation energy of KK100

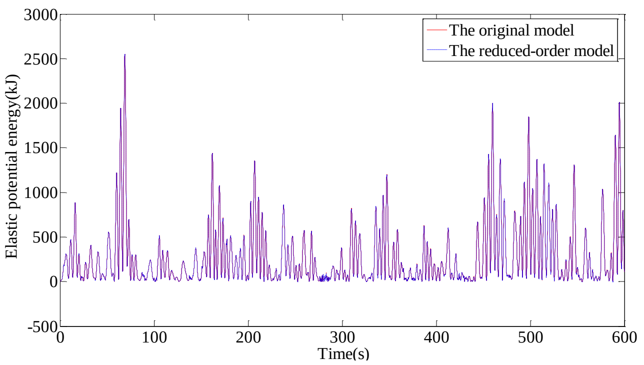

Fig. 11 The total elastic potential energy of KK100

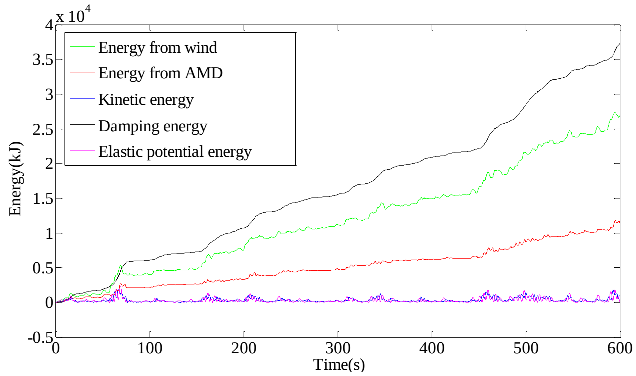

Fig. 12 The energy distribution of the AMD control system in KK100

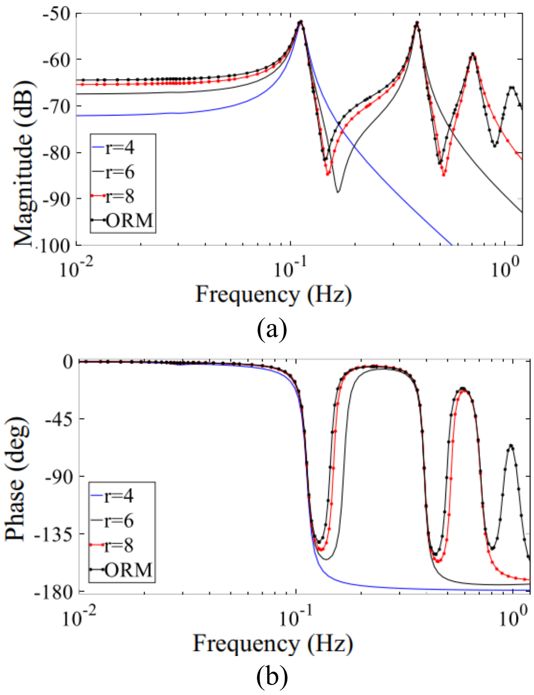

Fig. 13 The displacement transfer functions of the bottom floor of the experimental system under different retained orders, (a) the magnitude and (b) the phase

Table 5 The modal frequencies of the experimental frame

Mode number	Modal frequencies (Hz)			
	Original model	r=4	r=6	r=8
1	0.1354	0.1391	0.1368	0.1359
2	0.4634	--	0.4773	0.4657
3	0.8599	--	--	0.8630
4	1.2723	--	--	--

control system improves the damping dissipation energy capacity of high-rise buildings greatly.

4. Experimental verification

The experimental system consists of a four-storey frame and an AMD control device installed on the 4th floor (Teng *et al*. 2016). To validate the efficiency of the above method, the reduced-order controller by the improved BT method is applied to the experimental system. The full-order model of the experimental system is 10 (2×5), which includes a four-storey frame with an AMD system. The magnitudes of the displacement transfer functions of the bottom floor of its reduced-order models are shown in Fig. 13. In this figure, ORM means the structure retains the original model (10 orders), while r is the retained orders of 4, 6 and 8. Considering the structural frequency range, the part between 0.01 Hz and 2 Hz is shown in the figures. Through the reduced-order process, the first four modal frequencies of different systems are compared in Table 5. The original model used in the frequency domain response analysis is modified by a modal test. For the original model, the mass matrix and stiffness matrix are two important parameters. In the experimental system, the diagonal element of its mass matrix is the mass of each floor or auxiliary mass; the stiffness matrix is calculated based on its structural finite

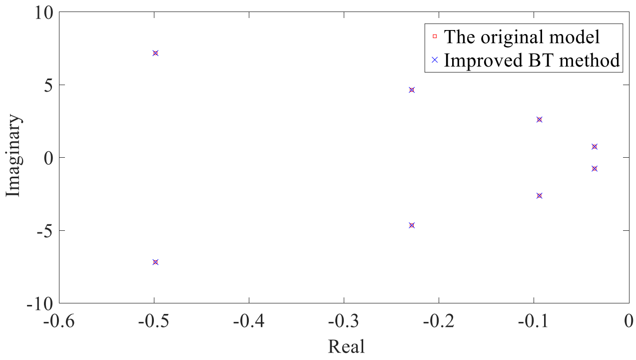

Fig. 14 The poles of the original model and the reduced-order models of the experimental system

element model, and then adjusted according to the measured natural frequencies, which are determined based on a modal test.

From Fig. 13 and Table 5, with the increase of the retained orders, the difference between the original model and the reduced-order model becomes smaller. The dynamic characteristics of the frame are mainly determined by the first few modes of the original structure that is continuous and with a large modal mass participating ratio. For the overhead frame, it is suggested to take 6 retained orders which mean the first three modes of the frame are retained. Meanwhile, the modal mass participation ratio of the frame is 0.9452, and the model-reduction accuracy is 90%.

The poles of the experimental system after using the original model and the reduced-order model obtained by the improved BT method are shown in Fig. 14. The pole positions of the balanced realization system are similar to those of the original system, indicating that the non-singular transformation does not change the system dynamic characteristics.

Under the excitation load which has a frequency of 1 Hz and a peak value of 45.89 N, the structural responses of different systems are shown in Fig. 15, and the corresponding control effects and its AMD parameters are

Table 6 The control effectiveness of the structural responses

Index		No control	The original control		The reduced-order control	
			Response	Reduction (%)	Response	Reduction (%)
Maximum displacement (m)	The 2nd floor	0.0158	0.0108	31.6456	0.0108	31.6456
	The 3rd floor	0.0231	0.0157	32.0346	0.0156	32.4675
	The 4th floor	0.0267	0.0182	31.8352	0.0180	32.5843
Maximum acceleration (m/s^2)	The 2nd floor	0.1174	0.0386	67.1210	0.0308	73.7649
	The 3rd floor	0.1247	0.0836	32.9591	0.0781	37.3697
	The 4th floor	0.1495	0.0561	62.4749	0.0478	68.0268
Maximum control force (N)		—	14.7916	—	15.2265	—
Maximum stroke (cm)		—	16.79	—	17.41	—

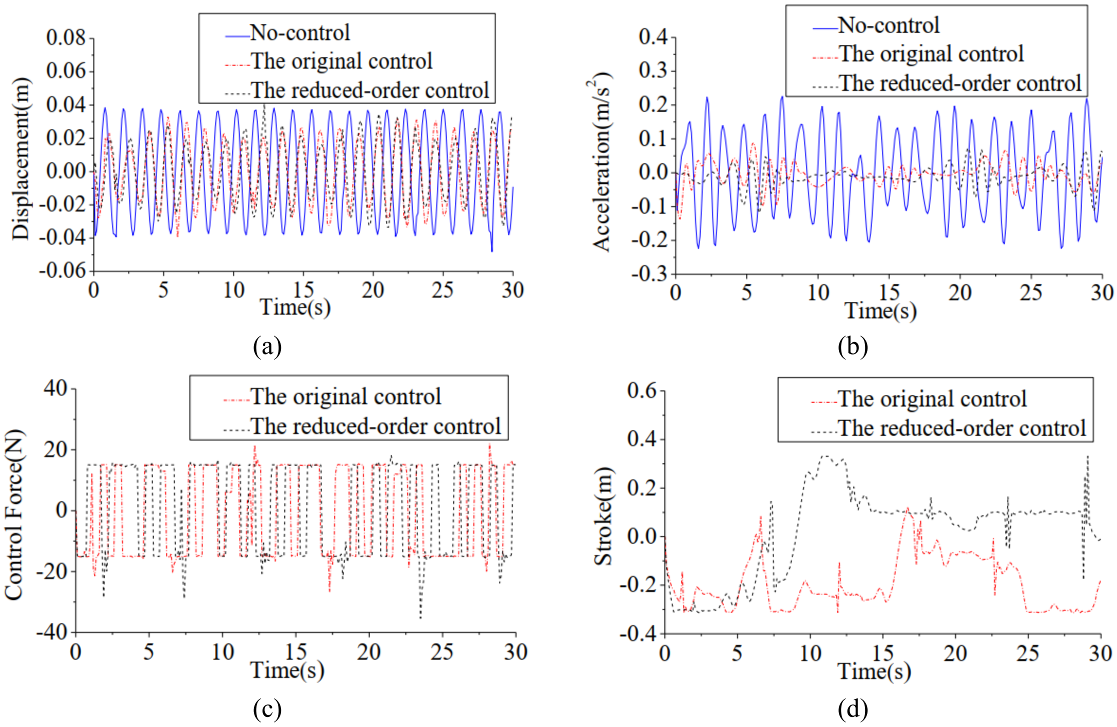

Fig. 15 The comparison of the structural responses of the 4th floor and the AMD parameters of the experimental system: (a) the displacement, (b) the acceleration, (c) the control force, (d) the stroke

listed in Table 6. The test duration of each scenario is 300s. Table 6 presents the root mean square values of the data, and the figures only give the time-history data in 30s.

From Fig. 15 and Table 6, the reduced-order controller based on the improved BT method suppresses structural responses effectively. The control effects and the AMD parameters of the reduced-order system are relatively close to the original system. In particular, the maximum variations of the displacement and acceleration control effects between two different systems are only 0.7491% and 6.6439%, and the AMD parameters of the reduced-order controller decrease by 0.4349 N and 0.62 cm. Under a sinusoidal excitation, the dynamic responses should be consistent with the excitation and obey the sine law. In fact, due to several factors, such as the interaction between the control system and the structure, the coupling between the horizontal and vertical vibrations of each floor, interference signals, unsmooth support track and uneven magnetic field between the rotor and stator, the structural response does not completely obey to the sine law, and its maximum amplitude fluctuates slightly. Since a state observer used acceleration signals to calculate control forces, the acceleration control effects are better than the displacement control effects. Acceleration control needs the control forces with a relatively high frequency, which creates the high-order modes. Meanwhile, the AMD device is placed on the 4^{th} floor of the structure, and the 3^{rd} floor has an opposite high-order phase with the 2^{nd} or 4^{th} floors. Therefore, its control effects are less than those on the 2^{nd} or 4^{th} floors.

5. Conclusions

A long control-force calculation time has a negative influence in AMD control systems. To address the issue, the paper has presented a new reduced-order controller. Several model-reduction methods have been compared and analyzed. Then, an improved reduced-order model that retains the abandoned modal information of its original model is proposed based on the dynamic characteristics of high-rise buildings. Finally, a new reduced-order controller is designed for a numerical example and an experimental system. Based on the results, the following conclusions can be drawn.

• The classical BT method retains the low-order vibration modes with a large modal mass participating ratio, and it is suitable for the model-reduction of high-rise buildings. The retained order of the reduced-order model is determined according to the model-reduction accuracy and the modal mass participating ratio of high-rise buildings.

• The dynamic characteristics of high-rise buildings are controlled by their low-order vibration modes. The classical BT method retains the low-order modal information, and the corresponding reduced-order model can better reflect the dynamic responses of the original model.

• Compared with the classical BT method, the reduced-order model obtained by the improved BT method has a higher accuracy. The model can better retain the abandoned structural modal information, and its acceleration transfer functions are more precise with the original model at a low frequency than that of the model obtained by the classical BT method.

• The dynamic responses of the reduced-order model obtained by the improved BT method are basically close to those of the original model. The improved model is used to design a reduced-order control system. The new controller suppresses wind vibration responses effectively, and it has reasonable AMD parameters and a short calculation time.

Acknowledgments

The research described in this paper was financially supported by the Funds for Creative Research Groups of National Natural Science Foundation of China (Grant No. 51921006), the National Natural Science Foundations of China (Grant Nos. 51978224 and 52008141), the China Postdoctoral Science Foundation Grant (Grant No. 2019M651291), the Hong Kong Scholars Program (Grant No. XJ2019039), the National Major Scientific Research Instrument Development Program of China (Grant No. 51827811), and the Shenzhen Technology Innovation Programs (Grant Nos. JCYJ20170811160003571 and JCYJ20180508152238111).

The authors declare that there is no conflict of interest regarding the publication of this paper.

References

Azam, S.E. and Mariani, S. (2013), "Investigation of computational and accuracy issues in POD-based reduced order modeling of dynamic structural systems", *Eng. Struct.*, **54**, 150-167. https://doi.org/10.1016/j.engstruct.2013.04.004.

Bigdeli, Y. and Kim, D. (2017), "Development of energy-based neuro-wavel*et al*gorithm to suppress structural vibration", *Struct. Eng. Mech.*, **62**(2), 237-246. https://doi.org/10.12989/sem.2017.62.2.237.

Boo, S.H. and Lee, P.S. (2017), "A dynamic condensation method using algebraic substructuring", *Int. J. Numer. Meth. Eng.*, **109**(12), 1701-1720. https://doi.org/10.1002/nme.5349.

Chen, C.J., Li, Z.H., Teng, J., Hu, W.H. and Wang, Y. (2017), "An observer-based controller with a LMI-based filter against wind-induced motion for high-rise buildings", *Shock Vib*., 1-18. https://doi.org/10.1155/2017/1427270.

Hartmann, C., Vulcanov, V.M. and Schutte, C. (2010), "Balanced truncation of linear second-order systems: a hamiltonian approach", *Multiscale Model Simul*., **8**(4), 1348-1367. https://doi.org/10.1137/080732717.

Jiang, J.W., Zhang, P., Patil, D., Li, H.N. and Song, G.B. (2017), "Experimental studies on the effectiveness and robustness of a pounding tuned mass damper for vibration suppression of a submerged cylindrical pipe", *Struct. Control Hlth*., **24**, e202712. https://doi.org/10.1002/stc.2027.

Jin, C.Y., Ryu, K.H., Sung, S.W., Lee, J. and Lee, I.B. (2014), "PID auto-tuning using new model reduction method and explicit PID tuning rule for a fractional order plus time delay model", *J. Proc. Contr*., **24**(1), 113-128. https://doi.org/10.1016/j.jprocont.2013.11.010.

Klis, D., Farle, O. and Dyczij-Edlinger, R. (2016), "Model-order reduction for the finite-element boundary-element simulation of eddy-current problems including rigid body motion", *IEEE T. Magnetic.*, **52**, 72004043. https://doi.org/10.1109/TMAG.2015.2482541.

Koreck, J. and von Estorff, O. (2015), "Reduced order structural models for the calculation of wet contact forces due to impacts in hydraulic valves", *Meccanica*, **50**(5), 1387-1401. https://doi.org/10.1007/s11012-014-0097-5.

Laub, A.J., Heath, M.T., Paige, C.C. and Ward, R.C. (1987), "Computation of system balancing transformations and other applications of simultaneous diagonalization algorithms", *IEEE T. Automat. Contr*., **32**(2), 115-122. https://doi.org/10.1109/TAC.1987.1104549.

Li, B., Dai, K., Li, H., Li, B. and Tesfamariam, S. (2019), "Optimum design of a non-conventional multiple tuned mass damper for a complex power plant structure", *Struct. Infrastruct. E*, **15**(7), 954-964. https://doi.org/10.1080/15732479.2019.1585461.

Li, C.X., Li, J.H. and Qu, Y. (2010), "An optimum design methodology of active tuned mass damper for asymmetric structures", *Mech. Syst. Signal Pr*., **24**(3), 746-765. https://doi.org/10.1016/j.ymssp.2009.09.011.

Li, C.X. and Qu, W.L. (2004), "Evaluation of elastically linked dashpot based active multiple tuned mass dampers for structures under ground acceleration", *Eng. Struct*., **26**(14), 2149-2160. https://doi.org/10.1016/j.engstruct.2004.07.019.

Li, C., Yu, Z., Xiong, X. and Wang, C. (2009), "Active multiple-tuned mass dampers for asymmetric structures considering soil-structure interaction", *Struct. Control Hlth*., **17**(4), 452-472. https://doi.org/10.1002/stc.326.

Li, Z.H., Chen, C.J., Teng, J. and Wang, Y. (2018), "A compensation controller based on a regional pole-assignment method for AMD control systems with a time-varying delay", *J. Sound Vib*., **419**, 18-32. https://doi.org/10.1016/j.jsv.2017.11.055.

Louca, L.S. (2014), "Modal analysis reduction of multi-body systems with generic damping", *J. Comput. Sci*., **5**(3), 415-426. https://doi.org/10.1016/j.jocs.2013.08.008.

Mortezaie, H. and Rezaie, F. (2018), "Effect of soil in controlling the seismic response of three-dimensional pbpd high-rise concrete structures", *Struct. Eng. Mech.*, **666**(2), 217-227. https://doi.org/10.12989/sem.2018.66.2.217.

Pekar, L. and Matusu, R. (2018), "A suboptimal shifting based Zero-pole placement method for systems with delays", *Int. J. Control Autom*., **16**(2), 594-608. https://doi.org/10.1007/s12555-017-0074-6.

Qian, H., Li, H.N. and Song, G.B. (2016), "Experimental investigations of building structure with a superelastic shape memory alloy friction damper subject to seismic loads", *Smart Mater. Struct*., **25**, 12502612. https://doi.org/10.1088/0964-1726/25/12/125026.

Qu, C.X., Huo, L.S., Li, H.N. and Wang, Y. (2014), "A double homotopy approach for decentralized H-infinity control of civil structures", *Struct. Control Hlth*., **21**(3), 269-281. https://doi.org/10.1002/stc.1552.

Rowley, C.W. and Dawson, S. (2017), "Model reduction for flow analysis and control", *Annu. Rev. Fluid Mech.*, **49**(1), 387-417. https://doi.org/10.1146/annurev-fluid-010816-060042.

Shen, W.A., Zhu, S.Y., Xu, Y.L. and Zhu, H.P. (2018), "Energy regenerative tuned mass dampers in high-rise buildings", *Struct. Control Hlth*., **25**, e20722. https://doi.org/10.1002/stc.2072.

Teng, J., Xing, H.B., Lu, W., Li, Z.H. and Chen, C.J. (2016), "Influence analysis of time delay to active mass damper control system using pole assignment method", *Mech. Syst. Signal Pr*., **80**, 99-116. https://doi.org/10.1016/j.ymssp.2016.04.008.

Wang, J., Li, H., Li, L. and Song, G. (2009), "Nonlinear decentralized control of seismically excited civil structures", *Proceedings of the SPIE - The International Society for Optical Engineering*, **7288**, 72882E. https://doi.org/10.1117/12.816460.

Wang, Y.N., Palacios, R. and Wynn, A. (2015), "A method for normal-mode-based model reduction in nonlinear dynamics of slender structures", *Comput. Struct.*, **159**, 26-40. https://doi.org/10.1016/j.compstruc.2015.07.001.

Xu, H.B., Zhang, C.W., Li, H. and Ou, J.P. (2014), "Real-time hybrid simulation approach for performance validation of structural active control systems: A linear motor actuator based active mass driver case study", *Struct. Control Hlth*., **21**(4), 574-589. https://doi.org/10.1002/stc.1585.

Yang, Y.Z. and Li, C.X. (2017), "Performance of tuned tandem mass dampers for structures under the ground acceleration", *Struct. Control Hlth*., **24**, e197410. https://doi.org/10.1002/stc.1974.

Zhang, C.W. and Ou, J.P. (2015), "Modeling and dynamical performance of the electromagnetic mass driver system forstructural vibration control", *Eng. Struct*., **82**, 93-103. https://doi.org/10.1016/j.engstruct.2014.10.029.

Zhang, P., Song, G.B., Li, H.N. and Lin, Y.X. (2013), "Seismic control of power transmission tower using pounding TMD", *J. Eng. Mech*., **139**(10), 1395-1406. https://doi.org/10.1061/(ASCE)EM.1943-7889.0000576.

Zhang, Z., Chen, J. and Li, J. (2014), "Seismic control of power transmission tower using pounding TMD", *J. Eng. Mech*., **139**(10), 1395-1406. https://doi.org/10.1061/(ASCE)EM.1943-7889.0000576.

Zhou, H.J., Huang, X.G., Xiang, N., He, J.W., Sun, L.M. and Xing, F. (2018). "Free vibration of a taut cable with a damper and a concentrated mass", *Struct. Control Hlth*., **25**, e225111. https://doi.org/10.1002/stc.2251.

Zhou, H.J., Qi, S.K., Yao, G.Z., Zhou, L.B., Sun, L.M. and Xing, F. (2018), "Damping and frequency of a model cable attached with a pre-tensioned shape memory alloy wire: experiment and analysis", *Struct. Control Hlth*., **25**, e21062. https://doi.org/10.1002/stc.2106.

Zhu, S.Y., Shen, W.A. and Xu, Y.L. (2012), "Linear electromagnetic devices for vibration damping and energy harvesting: Modeling and testing", *Eng. Struct*., **34**, 198-212. https://doi.org/10.1016/j.engstruct.2011.09.024.

PL